Diachronic Climatic Impacts on Water Resources

with Emphasis on the Mediterranean Region

Edited by

Andreas N. Angelakis
National Foundation for Agricultural Research
Institute of Iraklio
71110 Iraklio, Greece

Arie S. Issar
Ben-Gurion University of the Negev
The Jacob Blaustein Institute for Desert Research
Desert Hydrology Unit
Sede Boker Campus, 84990 Israel

Springer
Published in cooperation with NATO Scientific Affairs Division

CHAPTER 11

CATCHMENT HYDROLOGICAL SENSITIVITIES TO CLIMATE CHANGES

DIONYSIA G. PANAGOULIA

Division of Water Resources, Hydraulic and Maritime Engineering,
Department of Civil Engineering, National Technical University of Athens,
5 Iroon Polytechniou, 15780 Athens, GREECE

11-1. INTRODUCTION

While climate changes over periods of thousands of years are well documented, hydrologists were rather reluctant to agree for as long as a decade (1960 to 1970) as to whether changes (signals) within typical water resources systems design periods (100 years or less) can indeed be distinguished from random variations (noise) in a physical hydrological time series (US. National Academy of Sciences, 1977). The advent of general circulation models (GCMs) over the last decade and consensus about the direction of future global climate change threw abundant light on the controversial theme, thus making acceptable the aspect that climate change does exist.

The continued burning of fossil fuels, plus deforestation and changes in use of land (converting it to buildup and industrial areas), let alone the increased use of nitrogen fertilizers, as well as large nuclear eruptions and primarily atmospheric pollution, have increased the concentrations of carbon dioxide and other trace gases (e.g. CH_4, N_2O, CFC-11, CFC-12) by about 20% over the last one 100 years. It is expected during the next 50-80 years (until 2070) that these activities will result in doubling the concentration of CO_2 in the atmosphere (US National Academy of Science, 1983; MacCracken and Luther, 1986; Manabe and Wetherald, 1985; Mitchell and Qingcum 1991) and cause through green house effect a gradual warming up of the Earth. By varying the level of carbon dioxide concentration in GCMs simulations, the models can provide quantitative estimates (predictions) of climate and hydrology variables for any level of CO_2 and its possible doubling (experiment of CO_2 doubling).

A GCM solves numerically the equations of mass, energy, momentum and state on a global grid of cells (Hansen *et al.*, 1983; 1988; Mitchell and Qingcuì, 1991). But, this spatial scale of the GCM outputs is inadequate for catchment hydrological simulation. The GCM predictions are provided as spatial averages over areas of the order of 10^4-10^5 km^2 (macroscale), where the fundamental differential equations of the continuum hydro- and

NATO ASI Series, Vol. I 36
Diachronic Climatic Impacts on Water Resources
Edited by Andreas N. Angelakis and Arie S. Issar

thermo- dynamics can conserve a real-world validity in contrast to the validity of these equations when they are applied to the hydrological modelling of a catchment (meso-micro scale simulation) (Becker and Nemec, 1987). Furthermore, it is doubtful whether GCM predictions on time scales shorter than one month do reflect the natural variability of field data, because these predictions represent grid-cell averages. On the other hand, all the climate models, including the better parameterized ones (GCMs), give different values of climate variable changes and not a single reliable estimate that could be advanced as a deterministic forecast for hydrological modelling.

The study of the hydrological system sensitivities to changes in meteorological inputs requires these inputs to be specified on a time step appropriate for conceptual catchment simulation to event storms. This is because the transfer function of rainfall to runoff is not linear, also because the infiltration and evapotranspiration processes, that play a major role in catchment runoff determination, are highly dependent on the storages and movement of water within the soil during storm occurences, as well as on the soil moisture state at the beginning of storm (determination of soil moisture capacities).

The operation of soil moisture system requires daily, hourly or even shorter time scales, depending on the size of the river basin. The GCM outputs can be represented on daily or shorter time steps, but it is not clear whether the results with these short scales properly reflect the short term dynamics of the atmospheric circulation process (Lettenmaier and Gan, 1990).

Since we have yet to achieve an appropriate space-time coupling between GCMs outputs (e.g. temperature, precipitation, reference evaporation, etc.) and hydrological models, we thought, for hydrological purposes, of adjusting the present day surface meteorological data to account for scenarios of meteorological variable long-term changes based on GCM predictions.

Yet, any calibration for climate studies demands accurate and physical climatic information (Hutchinson, 1990, and Wallis *et al.*, 1991). This information is not so easy to obtain in mountainous regions where high slopes and strong winds do affect the measurement of true precipitation. In addition, harsh conditions cause instruments to malfunction more frequently, thereby leading to gaps in the records, as well as to nonhomogeneity when instruments have to be replaced and/or recalibrated.

The sensitivity of water resource systems to climate variations was first studied by Nemec and Schaake (1982) for two river basins in USA. Nemec and Schaake introduced the global climate change (climate variations) by hypothetical scenarios of changes in precipitation (±10%, ±25%) and temperature (±1°C, +3°C), the latter converted into changes in reference evaporation (±4%, +12% Budyko- relation). They did not study snowcovered basins and deal with other catchment hydrological processes than runoff.

Subsequently, Lettenmaier and Gan (1990) investigated the hydrological effects of

four subbasins in the Sacramento-San Joaquin river basin (California) for increases in temperature and reference evapotranspiration, as well as changes in precipitation that resulted from GFDL (Fluid Dynamics Laboratory), GISS (Goddard Institute for Space Studies), and OSU (Oregon State University) model scenarios.

The studies of Nemec and Schaake (1982) and Lettenmaier and Gan (1990) did not actually face the problem of incomplete meteorological point data integration for climate change adjustment. This difficult problem was dealt with in studies of Panagoulia.

So, the present chapter has been produced from a series of papers (Panagoulia, 1990, 1991a,b, 1992a,b, and 1993a,b) which deal with the long-term hydrological sensitivities (snow water equivalent, runoff, actual evapotranspiration and soil moisture) of a medium-sized mountainous catchment (in our case the Mesochora catchment in Central Greece) to hypothetical (given as range of changes in long- term average values of meteorological variables) and GISS-modelled climate changes. The used meteorological data included incomplete point values of daily precipitation and min-max temperature. In order to preserve the physical nature of climatic information and avoid the errors caused by the interpolation techniques (Georgakakos and Krajewski, 1991; Wallis *et al.*, 1991), we would rather not estimate the unavailable values, but integrate instead the existing ones for areal variation and change pro rata with elevation.

11-2. CATCHMENT FEATURES AND CLIMATE CHANGE SCENARIOS

The Mesochora catchment (632.8 km^2) lies in central mountain region of Greece and extends nearly 32 km from north (39° 42′) to south (39° 25′) with an average width of about 20 km (Fig. 11-1). The Pindus Mountains, with peak elevations of about 2300m, form the western boundary of the catchment, while the eastern one is formed by Koziakas mountains with peaks of about 2000m. Inside, the catchment presents intense topography with strong interchanges of lower and higher elevations. The mean elevation of catchment is 1390 m. The network of meteorological stations installed in and around the catchment is relatively dense, but 3.5% of daily precipitation values and 15.5% of daily min-max temperature values were missing for the 15-year period used in this study.

The climate in the Mesochora catchment is elevation-dependent, with hot summers and mild winters at low elevations and mild summers and cold winters higher up. Because of its high mean elevation, its hydrology is controlled by snowfall and snowmelt. The mean annual precipitation of catchment (weighted average over elevation bands) is 1898mm, and most of precipitation falls as snow at the higher elevations. The mean annual runoff of the catchment is about 1170 mm (or 23.5 m^3/s). The mean January and July daily temperatures (weighted average over elevation bands) are:

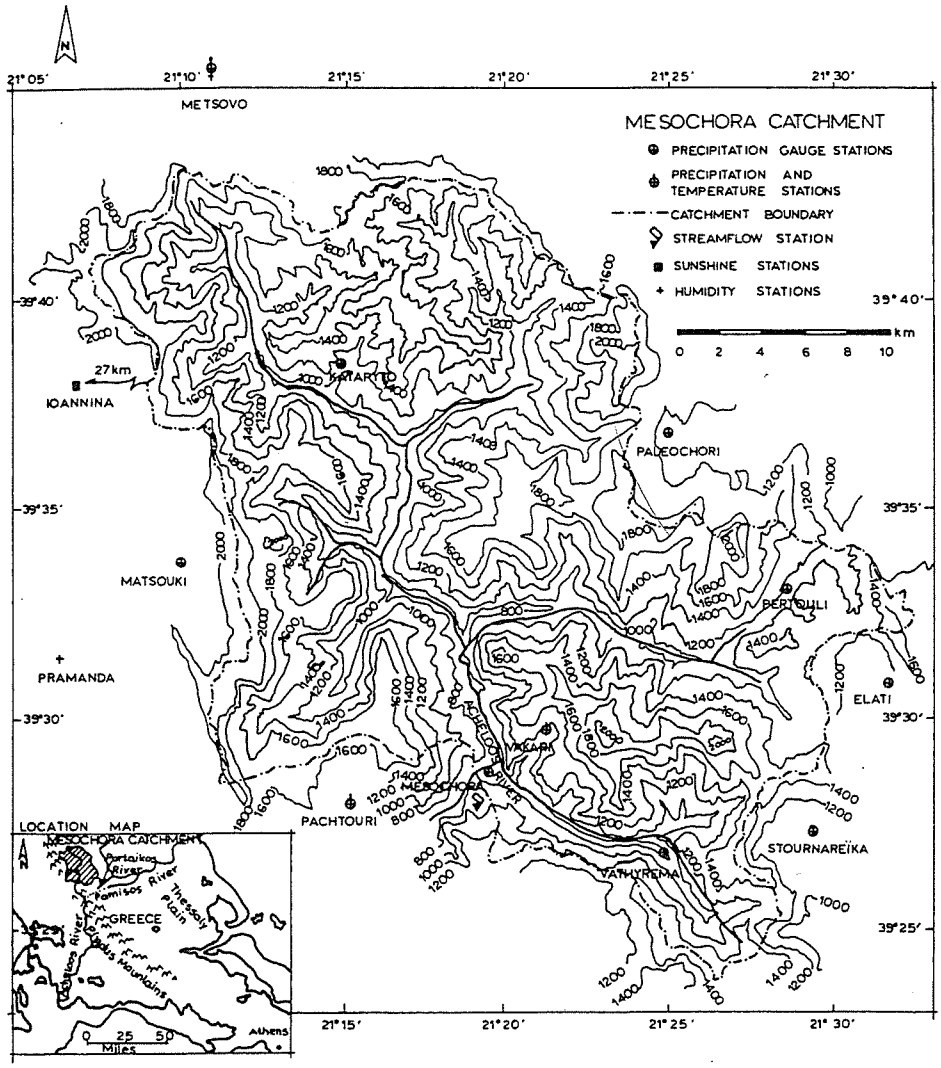

Figure 11-1. The Mesochora catchment, Greece. Topography and hydrometeorological stations

MEAN DAILY TEMPERATURE [^{0}C]		
	JANUARY	JULY
Daily Average	0.100	17.53
Minimum	-3.511	11.43
Maximum	3.711	23.63

The soils of the catchment have been formed from decayed hard limestone and flysch. They are varied, but generally permeable. Mesochora, which constitutes the upper drainage catchment of Acheloos river, has a great singificance for Greece because the river will be partially diverted at the outfall of the Mesochora catchment through Pindus mountains to irrigate the arid Thessaly Plain. It is the largest construction project in Greece including five dams (one is Mesochora's), 40 miles of large tunnels and about 8000 miles of buried irrigation piping.

In order to analyze the sensitivities of catchment hydrological regime to climate changes we used:

a) Fifteen hypothetical scenarios denoted as HYPO(Δ,T, ΔP), where ΔT is temperature increase by 1, 2, 4°C and ΔP is precipitation change by 0, ±10, ±20%, (Panagoulia 1991a)
b) Two GISS-predicted scenarios (with both monthly precipitation and temperature changes GISS(t,p), and with monthly temperature changes alone GISS(t,0)) (Panagoulia, 1992b).

The range of HYPO precipitation changes was selected from the recent climatological literature (U.S. National Academy of Sciences, 1983; Manabe and Wetherland, 1985 and MacCracken and Luther, 1986). Such scenarios have been previously used by Nemec and Schaake (1982), Revelle and Waggoner (1983) and Gleick (1986), for streamflow modelling under climate change conditions.

The HYPO temperature increases were taken from the range of 1.5 and 4.5°C temperature increase according to climate predictions for CO_2 doubling by the year 2070 (US. National Academy of Sciences, 1983; Dickinson, 1982, and Mac Cracken and Luther, 1986).

The GISS scenarios resulted from the GISS general circulation model which was developed by Hansen *et al.* (1983) of the Goddard Institute for Space Studies (NASA) in USA and keeps on ever since. This global model has realistic topography, 8°x10° (latitude x longitude) resolution in the horizontal, and nine layers in the vertical. The model simulates climate by solving the fundamental equations for conservation of mass, energy, momentum and water. The source terms in these equations incorporate numerical representations of the physical processes of radiation, turbulent transfers at the ground-atmosphere boundary, cloud formation, condensation of rain, and transport of heat by ocean boundary currents. A complete description of the model appears in Hansen *et al.* (1983).

However, there are many uncertainties in the modelling and parameterization of terms. Various processes, such as cloud feedbacks, are only crudely modelled. Initial conditions of temperatures and precipitation, i.e. control runs, are rather difficult to determine at all points. As a result, the model is unable to completely simulate the present climate, especially precipitation. When the initial parameterizations are modified by doubling atmospheric CO_2 concentration, any errors inherent in the initial model runs would probably occur in the $2xCO_2$ simulations. Another problem has to do with the relatively coarse resolution of the model outputs (8°x10°).

Despite the limitations on spatial resolution and hydrological parameterizations of the model, the outputs of GISS model, as well as certain other relative models, such as GFDL, OSU, and NCAR, are used for the formation of climate change scenarios for several reasons:

a) To evaluate the strengths and weaknesses of the hydrological mechanisms used by GCMs
b) To study the sensitivity of a watershed hydrological system to changes in meteorological variables.
c) To throw light on the required information about an appropriate coupling of physically-based hydrological models and climate models.

The model outputs or grid-cell data used in the study were obtained from the Goddard Institute for Space Studies and include average monthly air temperature and precipitation for a control run ($1xCO_2$) and the GISS $2xCO_2$ experiment. The runs were integrated for 35 years and the data provided are the average figures for each month over the last 10 years.

The data are the average values over an 8°X10° cell, with the data-point references located at the center of each cell. Data for all cells of the global grid were also obtained as above. Three cells were determined: one lies within Greece, and two are adjacent. The center data of the cell that belongs to Greece were interpolated, using the center data of the other two cells, to latitude 39°34′N and longitude 21°19′E, which is approximately the centroid of the Mesochora catchment. The temperature difference between the $2xCO_2$ and control run on a monthly basis yielded the monthly temperature change scenarios (ranging from 3.37 to 4.98°C), while the ratio of the $2xCO_2$ monthly precipitation to the control run monthly precipitation provided the scenario of relative climate change (ranging from 0.925 to 1.487).

11-3. METHODOLOGY

The methodology of conceptual catchment simulation was adopted in this study for reasons of detailed representation of a medium-sized catchment (Panagoulia and Dimou, 1994). Actually, there were used the Snow Accumulation and Ablation model and the Soil Moisture Accounting model of US National Weather Service River Forecast System. Each of the models is described briefly in this section.

Snow Accumulation and Ablation Model

This model was developed by Eric Anderson within the US National Weather Service Hydrologic Research Laboratory (Anderson, 1973). This is a deterministic, conceptual model consisting of a set of equations which describe the accumulation and ablation of a snowpack. The model inputs are air temperature and precipitation at a six-hourly time step. In this study, daily precipitation was interpolated to six-hourly increments and six-hourly temperatures were estimated from daily temperature maxima and minima using equations furnished by Anderson.

The model can be summarized as follows. Accumulation of snowpack occurs when air air temperature, T_a, is less than the delineation temperature which can be 0°C or other. In the opposite case (T_a> delineation temperature) the model assumes that the precipitation is rain. The ablation of snowpack is controlled by the heat exchange at the air-snow interface. For heat exchange computations there are two basic conditions, namely:

- when the air is warm (T_a>0°C) in which case melt takes place at the snow surface, and
- when the air is too cold (T_a<0°C) for melt to occur. Furthermore, the melt is computed for rain or non-rain periods. For melt during rain periods the following assumptions are made:
  * there is no solar radiation
  * incoming longwave radiation is equivalent to blackbody longwave radiation at T_a
  * snow surface temperature is 0°C
  * the dew point is T_a
  * the rain temperature is T_a.

Under these assumptions, the amount of melting snowpack expressed as heat losses, ΔQ is:

$$\Delta Q = Q_n + Q_e + Q_h + Q_{px}$$

where

Q_n long wave radiation
Q_e latent heat transfer due to condensation
Q_h sensible heat transfer
Q_{px} heat transfer by rain water.

For melt during non-rain periods, the model checks whether the snowpack is isothermal at 0°C. If the snowpack is not isothermal, no melt occurs and the net heat flux is added to the heat content of the snowpack. If the snowpack is isothermal, and the air temperature is T_a>0°C, melt occurs at a rate proportionate to a seasonally varying melt factor and the difference between the air temperature and 0°C.

During non-melt periods (the model assumes T_a<0 °C), an antecedent temperature index, *ATI*, is used as an index to the temperature of the surface layer of

snowpack. The heat exchange is assumed proportional to the temperature gradient defined by current air temperature and the andecedent temperature index. The proportionality constant is a parameter "called the negative melt factor" which varies seasonally in the same way as does the melt factor used during non-rain periods.The model accounts for the areal extent of snow cover. During the periods of snow accumulation, this is assumed to be 100%. During periods of depletion, the model uses an areal depletion curve of snow, that is a function of the areal extent of snow cover versus the ratio of mean areal water equivalent to an index value, which is the smaller of the maximum water equivalent (since snow began to accumulate), or a preset maximum. The six major and six minor parameters of the snow model are described in the section of parameter estimation.

Soil Moisture Accounting Model

The model was developed by Burnash *et al.* (1973) and forms the basis of the US. National Weather Service's basic catchment hydrologic response model for operational forecasting. It is a deterministic, continuous, lumped-parameter conceptual model. The original model was designed for daily precipitation input but later versions allows finer time increments (6 hours or less). Input to the model is pseudoprecipitation (rain plus melt model output) and reference evaporation (actual or long-term average). The model is based on a system of percolation, soil moisture storage, drainage and evapotranspiration characteristics to represent the significant hydrologic process in a rational manner. The components of the soil moisture hydrological model is shown in Figure 11.2. As seen from this figure, the model is represented by an upper and lower zone. The upper zone is divided into tension water storage and free water storage for the permeable portion of the catchment. Tension water is considered as that water which is closely bound to soil particles. This water is available for evapotranspiration based on the upper zone soil moisture. Tension water storage should be filled up before moisture becomes available to enter the free water storage. Free water can descend to lower zone by percolation or move laterally to produce interflow. Percolation is controlled by the contents of the upper zone free water and the deficiency of lower zone moisture volume.

When the precipitation rate exceeds the percolation rate and the maximum interflow drainage capacity, then the upper zone free water capacity is filled completely, whereupon the excess raifall will result in surface runoff.

Lower zone consists of tension water storage and two free water storages. Again, the tension water is available for evapotranspiration. The two free water storages fill up simultaneously from percolated water and drain independently at different rate, giving a variable ground water recession. Direct runoff from impervious areas, surface runoff, interflow and base flow from lower zone contribute to generate the channel inflow. The model employs about 21 parameters. These are soil moisture storage parameters for

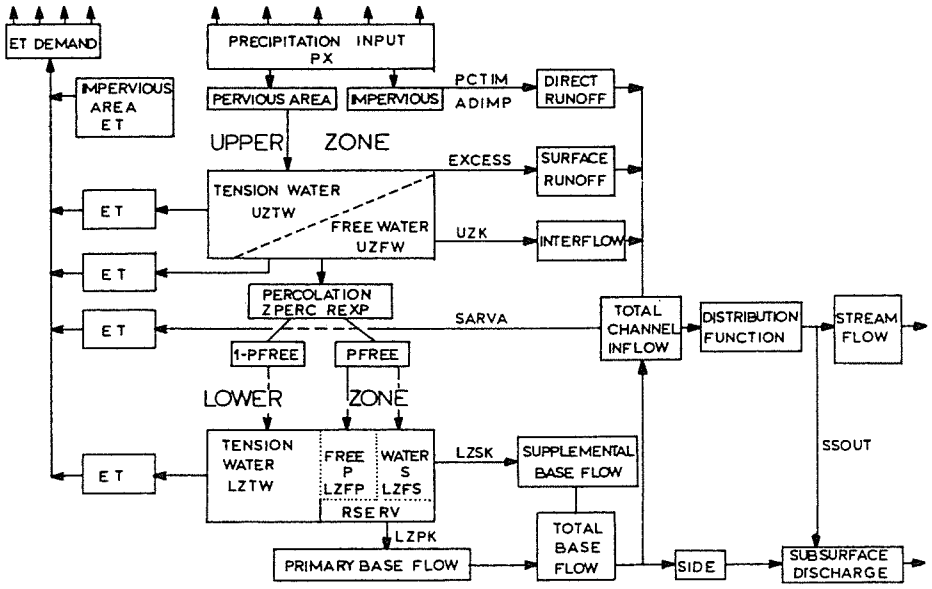

Figure 11-2. Soil moisture accounting model components

upper and lower zone, percolation parameters, catchment characteristics. These parameters are described in the section of parameter estimation. Some parameters can be estimated from semi-log plot of discharge or geographic maps of the study area.

11-4. HISTORICAL INPUT DATA

Three categories of stations and data, according to their use by the models, are hereby described. These are:

a) Precipitation and temperature stations with daily data
b) Temperature, sunshine, and humidity stations with monthly data
c) Streamflow station with daily data.

In addition, the methods used to average the station measurements data over area and elevation are described as well.

Precipitation and Temperature Stations Data

Eleven precipitation stations are installed within and around the Mesochora catchment, with the greater density at the lower part of the catchment (Fig. 11-1). The general characteristics of the stations for the study period (1972-1986) are presented in Table 11-1.

Table 11-1. Precipitation gauge stations by elevation zone, and temperature stations for the entire Mesochora catchment

Zone	Station	Station Elevation (m)	Zone Elevation Range (m)	Zone Median Elevation (m)	Zone Area %	Years of Record		
						Precipitation	Temperature max	min
Upper	Metsovo	1157	1580-2200	1830	30.54	15	14	15
	Katafyto	980				15		
	Palaiochori	1050				15		
Middle	Palaiochori	1050	1280-1580	1400	29.51	15		
	Matsouki	1079				15		
	Pertouli	1160				15		
Lower	Elati (Tyrna)	900	780-1280	1080	39.95	15		
	Vakari	1150				15	15	15
	Mesochora	780				15		
	Pachtouri	950				15	11	11
	Stournareika	860				15		
	Vathyrema	920				15		

The precipitation stations are consistent with and representative of the catchment, but in some precipitation records daily data are missing. We would rather not interpolate them for three reasons in the main:

a) In order to preserve the real nature of precipitation-temperature series elements.
b) In order to avoid the computing errors that are introduced by the estimation techniques of daily missing data (Linsley *et al.*, 1988).
c) Because these last techniques are applied to with difficulty and especialy so the multisite stochastic models.

Thus, the technique used to estimate the mean areal daily precipitation was a combinatorial one consisting of a similar Thiessen method plus station daily availability, and including elevation correction (Panagoulia, 1991a). The correction areal precipitation factor for a given elevation (e.g. midpoint catchment elevation) is obtained from the following algorithm.

$$p_e = [P + (e - e_{ws})p_f]/P \tag{11-1}$$

where

p_e = corrective precipitation factor for elevation e,
P = mean areal precipitation,
e_{ws} = weighted mean station elevation based on station daily availability,
p_f = variation rate of precipitation with elevation.

As regards the network of temperature stations there are three stations. One is installed inside the catchment, while the other two are installed outside it and present significant deficiencies of daily maximum and minimum data. The consistency of the data was checked by the double-mass curve on monthly basis (Anderson, 1973), and some deviations from straight line were observed for minimum data. The inconsistent data were corrected by applying an appropriate corrective factor of the order -0.6 to -1.0°C. For the implementation of consistency checking only, in the case of missing monthly minimum temperatures, these were interpolated by the long-term average values of their existing monthly data. The consistency checking of the corrected actual data did not show an absolute straight line in the double-mass curve diagram, but merely two or three hardly distinguishable parallel straight-lines. The technique used to estimate the mean areal maximum and minimum daily temperature was, also, a combinatorial one of a look like Thiessen method and station daily availability. The correction areal temperature factor for a given elevation is obtained from the following algorithm:

$$t_e = (e - e_{ws})\, t_f \qquad (11\text{-}2)$$

where

t_e = additive corrective temperature factor for elevation e
e_{ws} = weighted mean station elevation based on station daily availability
t_f = rate of temperature decrease with elevation (lapse rate).

Reference Evapotranspiration

In order to obtain the catchment reference evapotranspiration (RET), (Allen *et al.*, 1994; Doorenbos and Pruitt, 1977, and Jensen *et al.*, 1990) the sunshine, temperature and humidity data were considered. Their measurement stations are described in Table 11-2. The sunshine stations are outside the catchment, the Ioannina is at the north-west boundary of the catchment, while the M.Kerasia station is at the eastern boundary. The catchment sunshine is computed from the long-term monthly arithmetic average of the sunshine of the two stations. With the above manner was also calculated the catchment humidity from the two stations. The Pramanta station is installed outside the catchment near the western boundary.

The catchment temperature was estimated by the aforesaid Thiessen method combined with the monthly station availability. The areal temperature was corrected for catchment mean elevation by applying a monthly dependent lapse rate according to Equation 11-2. The long-term monthly mean catchment sunshine, temperature, and humidity were used as inputs to Penman equation which is given in Veihmeyer (1964) to estimate the catchment reference evapotranspiration.

Other inputs to Penman equation were the average wind speed, (200 miles/day), the monthly percent of reflecting surface and the solar radiation for the midpoint catchment latitude. The sunshine was entered to Penman equation as monthly ratio of duration of bright sunshine to maximum possible duration of bright sunshine.

Table 11-2. Sunshine temperature and humidity gauge stations of Mesochora catchment

Meteorological Variable	Station	Station Elevation (m)	Period of Records
Sunshine	Ioannina	483	1972-86
	M. Kerasia	560	1972-86
Temperature	Metsovo	1156	1961-86
	Vakari	1150	1972-86
	Pachtouri	950	1972-81
Humidity	Metsovo	1156	1970-86
	Pramanta	835	1970-86

Streamflow

The daily streamflow data of the Mesochora gauge station for the period 1972-86 were used in this study. Most of the streamflow records were complete, but some missing daily data were computed and included. For estimating the missing data, the Avlaki station was used as a backup station, while the average monthly streamflow for both stations was being computed. The Mesochora missing data were arrived at by multiplying the complete daily data of Avlaki station by the ratio of the monthly average streamflow (Mesochora/Avlaki).

11-5. MODEL CALIBRATION

The procedures used for models calibration (parameter estimation) and soil moisture accounting model verification are elaborated on as follows.

Snow Accumulation and Ablation Model Parameter Estimation

The mountainous catchment was divided into elevation zones, and the snowmelt model was applied to each zone separately, since low elevations are likely to receive rain, while higher elevations receive snow from the same storm. The weighted mean value of the pseudo-precipitation from all zones was treated as the mean areal precipitation which is the input to the Soil-Moisture Accounting model. In general, the

weighting factors used were equal to the ratios of the elevation zone subareas for the total catchment area.

The elevation bands were delineated as follows: First hypsometric curve (elevation versus area fraction) was developed. The catchment was then divided into three zones of area, depending on the elevation range, and the elevation of the midpoint of each band was identified (Table 11-1).

The snowmelt model was manually calibrated for the three elevation zones. According to available station data on that particular day, for every elevation zone, the precipitation-elevation correction factors p_e, were estimated through a trial and error approach, which was carried out concurrently with the calibration of Soil Moisture Accounting model. As with the function p_e, the lapse rate is usually nonlinear. It was found that average lapse rates for four periods (each 6 hours long) of each day is -0.80°C/100 m. The lapse rates, t_f and the temperature correction factors, t_e, were also estimated concurrently with the calibration of Soil model.

Seasonal melt factors were interpolated between *MFMAX* and *MFMIN* and estimated to 0.9 and 0.4 mm/°C/6 hours, respectively. *PXTEMP*, the temperature [°C] above, where precipitation was assumed to be rain was assumed to be 1°C for the first six months of calendar year, and 0°C for the rest ones. SI, the mean areal water-equivalent above which 100% areal snow cover always exist, was assumed to be 100mm. (See Table 11-3 for description and calibrated values of the snow-melt model parameters).

Soil Moisture Accounting Model Parameter Estimation

Parameter estimation for the soil moisture accounting model was based on a process of initial parameter estimation, as suggested by Peck (1976). The final values of parameters were obtained through manual model calibration on the Mesochora catchment. The description of model parameters and their final values are listed in Table 11-4. The model was calibrated for all the study period of from 1972 to 1986, which included dry, medium and wet years, so that the model could be subjected to a broad range of changes in conceptual storages.

The results of error analysis of daily flow, the three-day volume including peaks, as well as the comparison between simulated and observed flow components (Panagoulia, 1992a) showed that both hydrological models are capable of reproducing the observed streamflow (the snowmelt model indirectly, and the rainfall-runoff model directly). Also, the typical monthly simulation errors (monthly differences between simulated and observed streamflows), expressed in per cents of observed flows, were of the order of 10-15%, higher in low runoff months (August and September) and lower in high runoff months.

Table 11-3. Snow melt model parameter description and parameter calibrated values

Parameter	Description	Calibrated values
SCF	A multiplying factor to correct for gauge catch deficiency in the case of snowfall	1.10
MFMAX	Maximum melt factor during non-rain periods which occurs on June 21	0.90 mm/°C/6hr
MFMIN	Minimum melt factor during non-rain periods which occurs on December 21	0.40 mm/°C/6hr
UADJ	Average wind function during rain on snow periods	0.10 mm/mb/6hr
SI	Mean areal water-equivalent above which there is always 100% areal snow cover	100 mm
NMF	Maximum negative melt factor	0.12 mm_e/°C/6hr
TIMP	Antecedent temperature index parameter	0.30
PXTEMP	Temperature which delineates rain from snow	1.0 - 0°C
MBASE	Base temperature for snow melt computation during non-rain periods	0°C
PLWHC	Percent liquid-water holding capacity of ripe snow	0.05
PAYGM	Average daily ground at the snow-soil interface	0.020 mm
EFC	Percent area over which evapotranspiration occurs when there is 100% snow cover	0.61

Table 11-4. Soil moisture accounting model parameter description and parameter final values

Soil Moisture Phase	Parameters	Description	Final values
Direct runoff			
	PCTIM	Minimum impervious catchment	0.01
	ADIMP	Additional impervious catchment	0.01
	SARVA	Catchment covered by streams, lakes and riparian vegetation	0.0
Upper zone			
	UZTWM	Upper zone tension under capacity	4.50 cm
	UZFWM	Upper zone free water capacity	4.61 cm
	UZK	Daily upper zone free water drainage rate	0.57

Percolation			
	ZPERC	Proportional increase in percolation from saturated to dry condition	6.00
	REXP	Exponent affecting rate of change of percolation between wet and dry conditions.	1.80
Lower zone			
	LZTWM	Lower zone tension water capacity	25.00 cm
	LZFSM	Lower zone supplementary free water capacity	9.00 cm
	LZFPM	Lower zone primary freewater capacity	30.00
	LZSK	Daily lower zone supplementary free water drainage rate	0.15
	LZPK	Daily lower zone primary free water drainage rate	0.015
	PFREE	Percolation water fraction passing directly to lower zones free water	0.20
	RSERV	Fraction of lower zone free water unavailable for transpiration	0.10
	SIDE	Ratio of non-channel baseflow to channel baseflow	0.00
Initial water			
	UZTWC	Upper zone tension water content	4.50 cm
	UZFWC	Upper zone free water content	0.11 cm
	LZTWC	Lower zone tension water content	21.41 cm
	LZFSC	Lower zone supplementary free water content	0.088 cm
	LZFPC	Lower zone primary free water content	2.26 cm
	ADIMC	Tension water content of the additional impervious catchment	25.91 cm

Model Verification (robustness) for Climate Change Studies

The plot of the long-term annual mean catchment pseudo-precipitation (rain plus melt) (Fig. 11-3) reflected three distinct periods with different climate conditions. A modified differential split sample test was implemented in order to verify the ability of the model to respond, without significant deviation, to the three different climate periods. The model was run for each period separately, and the statistical variables: long-term annual mean runoff, standard deviation of annual runoff, standard error and correlation coefficient of monthly runoff, were accordingly computed (Table 11-5). The null hypothesis H_0 of the variable difference between two climate periods and any climate period and calibration period was also tested. The results for all variables fell within 95% of the critical region.

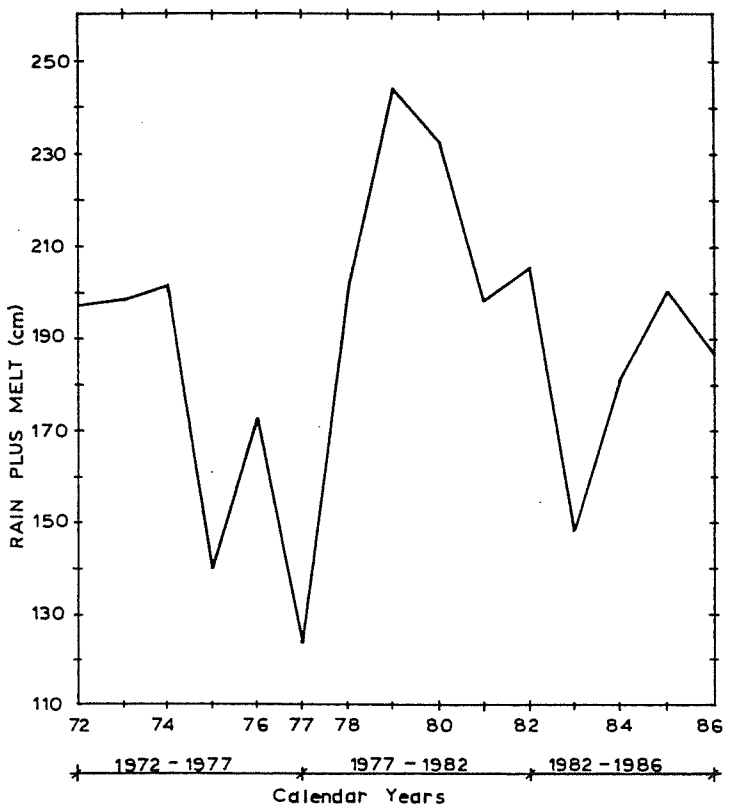

Figure 11-3. Annual pseudo-precipitation (rain plus melt) of the Mesochora catchment

Table 11-5. Values of statistical variables for climate periods and calibration period

Mesochora Catchment Pseudo-precipitation	Annual Runoff		Monthly Runoff	
Period	Average Value (cm)	Standard Deviation (cm)	Standard Error (cm)	Correlation Coefficient
Intense Descending	99.67	27.80	2.213	0.944
Intense Rising	128.32	45.63	2.940	0.961
Mild Descending	113.43	21.16	2.989	0.935
Calibration Period	119.23	30.16	2.581	0.954

11-6. ALTERED CLIMATE INPUTS

The historical input data were adjusted to reflect the altered climates simulated by each of fifteen HYPO and each of two GISS-conceived climate change scenarios. Particularly, the climate change applied to the historical time series: (a) daily precipitation, (b) daily minimum and maximum temperature, and (c) monthly temperature in order to be converted into changes of reference evapotranspiration. The description of the climate change and its implementation on each of the (a), (b), and (c) time series runs as follows.

a) Precipitation : All the daily values of the historical input precipitation series were multiplied for the HYPO changes by a uniform factor and for the GISS cases by the monthly precipitation ratio for CO_2 doubling and control runs.Thus, there resulted five altered daily precipitation series (time series scenarios) corresponding to the five climate change scenarios, and one series with zero precipitation change.

b) Temperature : The HYPO temperature increase scenarios were applied uniformly to both minimum and maximum daily values of the historical input temperature series, while the GISS-predicted monthly temperature differences between the CO_2 doubling and control run were added to the min/max daily values of the input historical temperature data as well. Thus, we obtained four altered daily temperature time series of minima and four of maxima, corresponding to the four temperature increase scenarios.

c) Reference Evapotranspiration : RET was computed on a monthly basis using the Penman equation, as a function of the meteorological variables: temperature, relative humidity, wind speed, relative sunshine, and mean solar radiation. Of these input variables, only temperature can be associated with climate changes, while the other variables are indirectly influenced by the climate change through a not well known mechanism that does not permit their change assessment. Therefore, in Penman's equation the only variable which was linked to climate change was the monthly temperature, while the rest were assumed not to be affected by it.

The monthly temperature increase scenarios were the same with those applied to daily time series because the mean monthly temperature is computed by averaging either the mean minimum and maximum daily temperature or three mean daily temperature values (8hr observations) by doubling the third temperature value (night's). Therefore, if the minimum and maximum daily temperature goes up by the same amount, this implies that during all hours of the day there will prevail the same temperature increase, a fact that identifies this increase with the mean monthly temperature, this regardless of the way it was actually computed. The monthly temperature increase scenarios were 1°C, 2°C, 4°C (HYPO case) and GISS-predicted for CO_2 doubling and control run.

The HYPO scenarios were applied uniformly to monthly values of the historical time series of catchment temperature and three altered monthly temperature time series (time

series scenarios) were obtained. These altered temperature time series were used as inputs to Penman equation which in its turn yielded three monthly time series of *RET* (time series reference evapotranspiration scenarios) corresponding to the three principal temperature increases. For the GISS cases the *RET* was also computed with the same equation for the monthly temperature data for the CO_2-doubling and control run.The monthly differences in *RET* were computed and these differences were added to the historical *RET* data. The long- term average of each monthly reference evapotranspiration series was used as input to soil moisture accounting model.

11-7. HYDROLOGICAL RESPONSE ANALYSIS

As described previously, the long-term hydrological response of the Mesochora catchment was simulated for climate regimes associated with a base case (nominally, present climate conditions, solid line in graphs), as well as fifteen hypothetical and two GISS-predicted climate change scenarios.

Because the snow accumulation and ablation model, as well as the soil moisture accounting model operate on daily or shorter time steps and all scenarios involved running both models for fifteen years, large amounts of computer output were generated. To simplify the analysis of the results that are reported as averages over the 15year simulation period, we selected the following simulated variables to describe the alternative hydrologies:

a) Monthly average snow water equivalent over catchment.
b) Monthly average catchment runoff.
c) Monthly average catchment evapotranspiration.
d) Monthly average catchment soil moisture storage in simulated zones.

For the seventeen climate change scenarios the (a) simulated variable yielded seventeen monthly snow water equivalent scenarios, the (b) plus seventeen monthly runoff scenarios, the (c) plus seventeen monthly evapotranspiration scenarios, and (d) seventeen monthly soil moisture storage for each of the five model moisture zones, resulting totally to one hundred and thirty six catchment hydrological response scenarios plus the eight ones of the base case (model outputs for present climate conditions, solid line in graphs). The hydrological scenarios of the above variables are plotted in Figures 4 to 11 and a brief interpretation of these figures follows.

Snow Water Equivalent

The long-term monthly snow water equivalent over the study catchment for all alternative climates is presented in Figure 11-4. There was a marked reduction in average snow water equivalent for all alternative scenarios. The GISS scenarios and the HYPO(4, all) produced the maximum reduction in snow water equivalent. They generally generated similar annual snow water equivalent hydrographs in the same

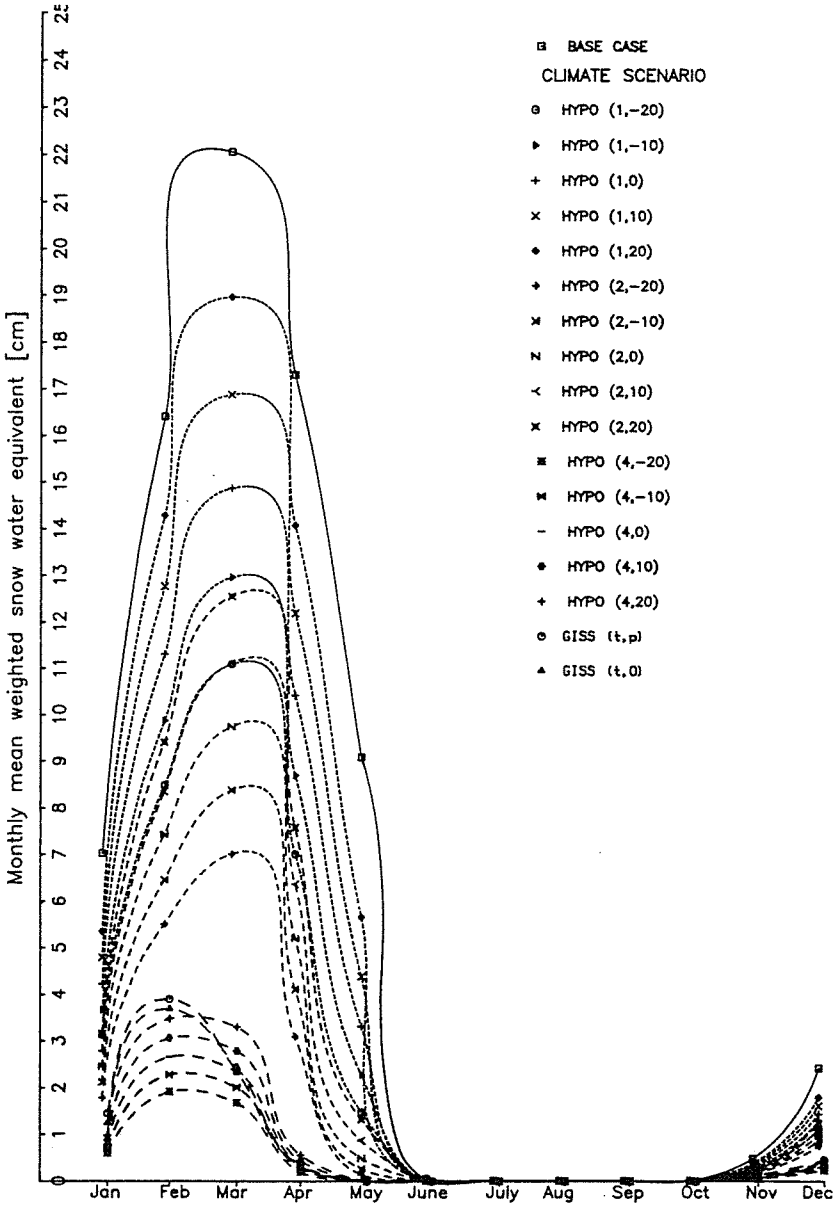

Figure 11-4. Mesochora catchment monthly mean snow water equivalent for the HYPO, GISS and base case climate scenarios

month of snow maximization, extinction and return. But there is a difference in snow water profiles: the HYPO(4, all) cases yielded hydrographs with obviously flatter crest than that of GISS ones. This is because the GISS- predicted climate changes have different monthly values, while those of HYPO are the same within the month. Searching, on a monthly basis, for equivalencies among all the scenarios, those characterized by 4°C increase appeared to be more similar. This is perhaps due to the fact that the average of the GISS monthly temperature increases is 3.94°C, a value which is approximately the same with that of HYPO(4, all) scenarios.

Runoff

Figure 11-5 shows significant changes in the seasonal distribution of Mesochora catchment runoff for all 17 climate scenarios. The effect of reduced snow storages and change in the timing of snowmelt (Fig. 11-4) are seen clearly in all runoff responses. The annual hydrograph peak shifted to earlier in the year because of a decrease in the amount of snowfall in relation to rainfall. The summer runoff went down considerably in GISS scenarios and 14 of the 15 HYPO cases. The summer runoff resulting from the scenarios HYPO(1, 20) went up a little due to the small increase of the temperature and large precipitation increase. The winter runoff increased in the two GISS scenarios and 10 of the 15 HYPO cases. It decreased in the case of the climate scenarios HYPO(1,10), HYPO(2,10) and HYPO(all, 20). For the April to August period the scenarios of HYPO(1,-20) and HYPO(2,-10) are similar to GISS(t, p).

Evapotranspiration

The actual evapotranspiration (*ET*) simulated by the soil moisture accounting model depends on soil moisture status, as well as on *RET*. Therefore, although *RET* increased for all months and climates (HYPO and GISS) due to temperature rise, the direction of change in *ET* varied from season to season. During the wet November-April period, *ET* remained unaffected by precipitation changes (Fig. 11-6), but increased in relation to base case *ET*. During the dry May-October period *ET* increased with precipitation increase and decreased with precipitation reduction.

The peak value of monthly *ET* occured in June for the base case and 9 of the 15 HYPO scenarios, while the other 6 scenarios (characterized by precipitation reduction), as well as the GISS climates peaked in May. The GISS scenarios as well as those of HYPO ones with minor precipitation reduction showed a flatter crest in the monthly distribution of *ET*. For the winter months the GISS scenarios are similar to HYPO(4, all).

Upper Zone Free Water

The free water contents in all three zones of the model are strongly and erratically influenced by HYPO and GISS scenarios, as well as from month to month under the

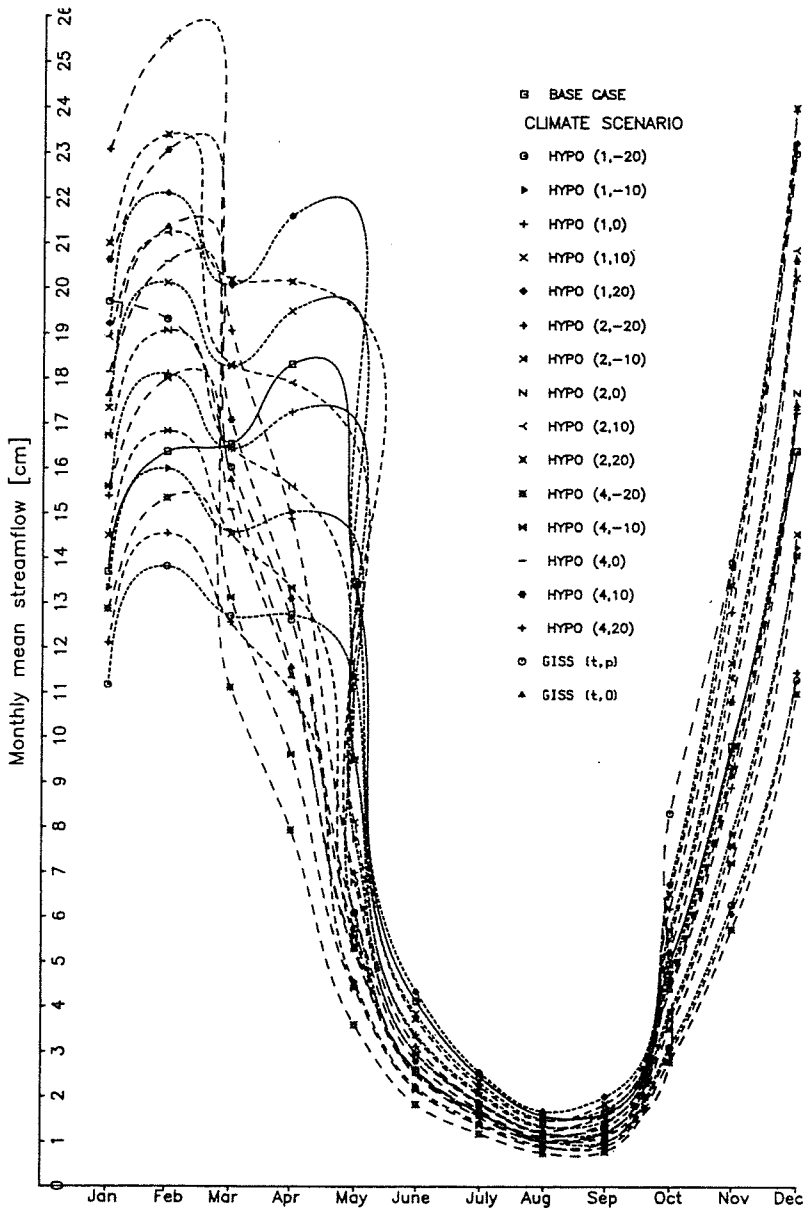

Figure 11-5. Mesochora catchment monthly mean runoff for the HYPO, GISS and base case climate scenarios

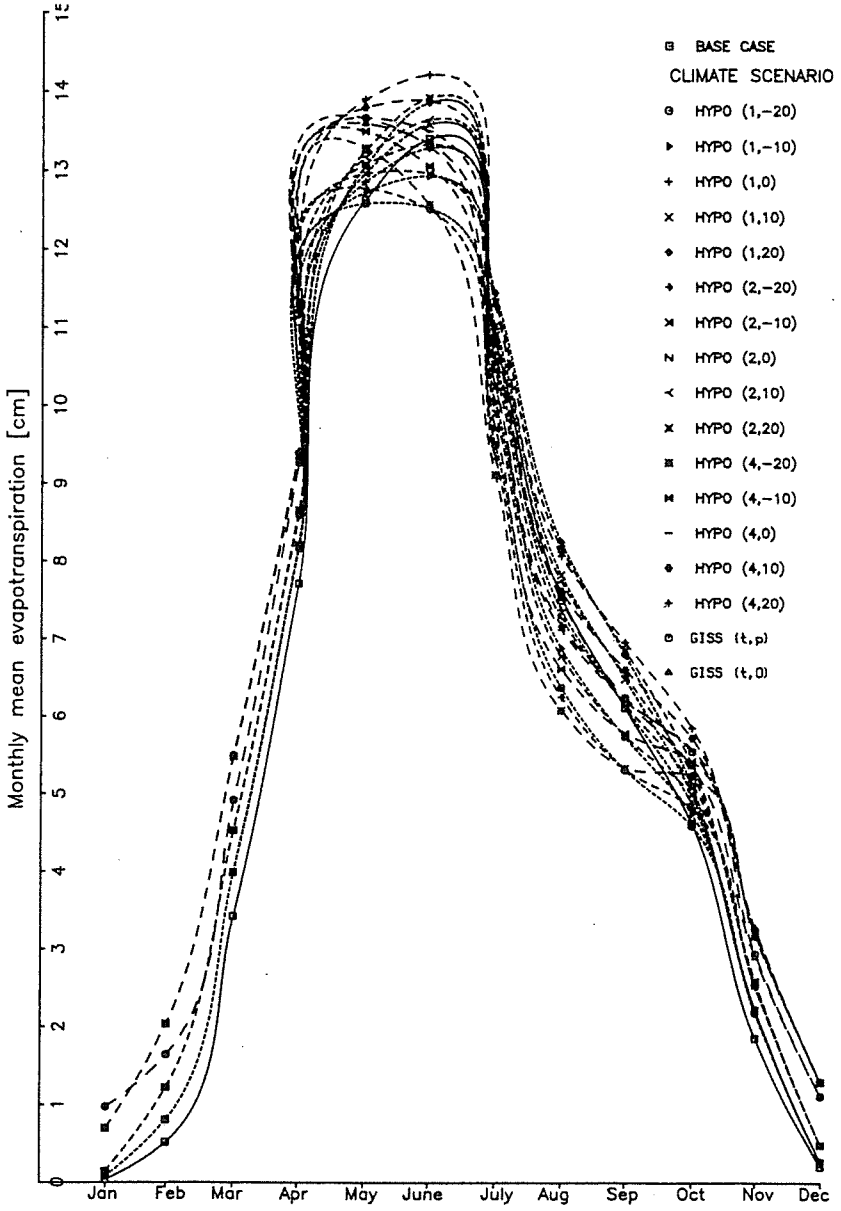

Figure 11-6. Mesochora catchment monthly mean evapotranspiration for the HYPO, GISS and base case climate scenarios

same scenario. Notwithstanding that, the free moisture content of the upper zone (Fig. 11-7) posted larger fluctuations than those of the lower zones (Figs 11-8 and 11-9). Indeed, it peaked in January for the drier HYPO climate scenarios and in December for the rest HYPO, GISS and the base case, while during the summer dry period (July-October), the upper zone free water went down for all HYPO and GISS cases.

Lower Zone Primary Free Water

The free moisture content of the lower primary zone (Fig 11-10) supplies the baseflow with larger amounts than those of lower supplement zone. It peaked in March for 13 of the 15 HYPO and GISS cases, while that of the base case reached its maximum in May. The other two scenarios HYPO(1,-20) and HYPO(1,-10) caused the primary free moisture content to come to a maximum in April. For all HYPO and GISS scenarios the primary free moisture was minimized in October.

Lower Zone Supplemental Free Water

For 12 of the 15 HYPO scenarios and GISS(t, 0) the supplemental moisture content (Fig. 11-11) peaked in March, while for the GISS(t, p), HYPO(2,-10), HYPO(4,-20) and HYPO(4,-10) the peak shifted to February. The GISS(t, 0) case appeared shifted earlier by one month from the peak month (April) for the base case. This content is minimized in August for HYPO and July-September period for GISS climate cases.

Upper Zone Tension Water

The moisture content of the upper tension zone (Fig. 11-8) is little affected by HYPO and GISS climate changes in winter period (December to February), while all the other months are affected much more. The tension moisture content of this zone is reduced for all months and its maximum fall occurs in May for both HYPO and GISS scenarios. The seasonal tension moisture profiles are very similar for both cases of HYPO and GISS scenarios.The fact of the considerable tension moisture reduction in spring and early summer months is to be attributed to snowmelt reduction that contributes to soil moisture.

Lower Zone Tension Water

The moisture content of the lower tension zone (Fig. 11-9) shows the same monthly distribution profile for both HYPO and GISS scenarios. The largest reduction in lower tension moisture occurs in October for the two GISS and HYPO(4,-20) scenarios. Generally, the larger lower zone tension moisture reductions appear shifted forward by two or three months compared with these of upper zone tension moisture storages.

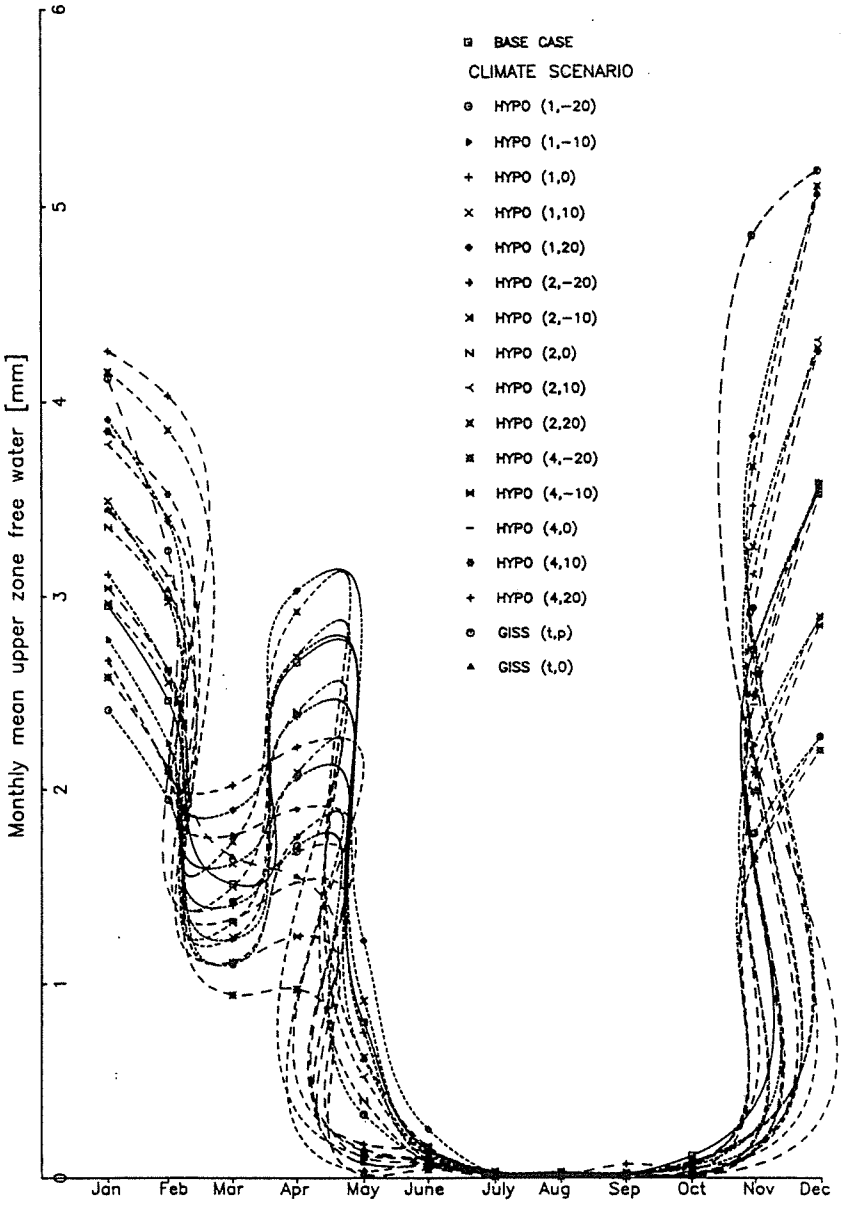

Figure 11-7. Mesochora catchment monthly mean upper zone free water for the HYPO, GISS and base case climate scenarios

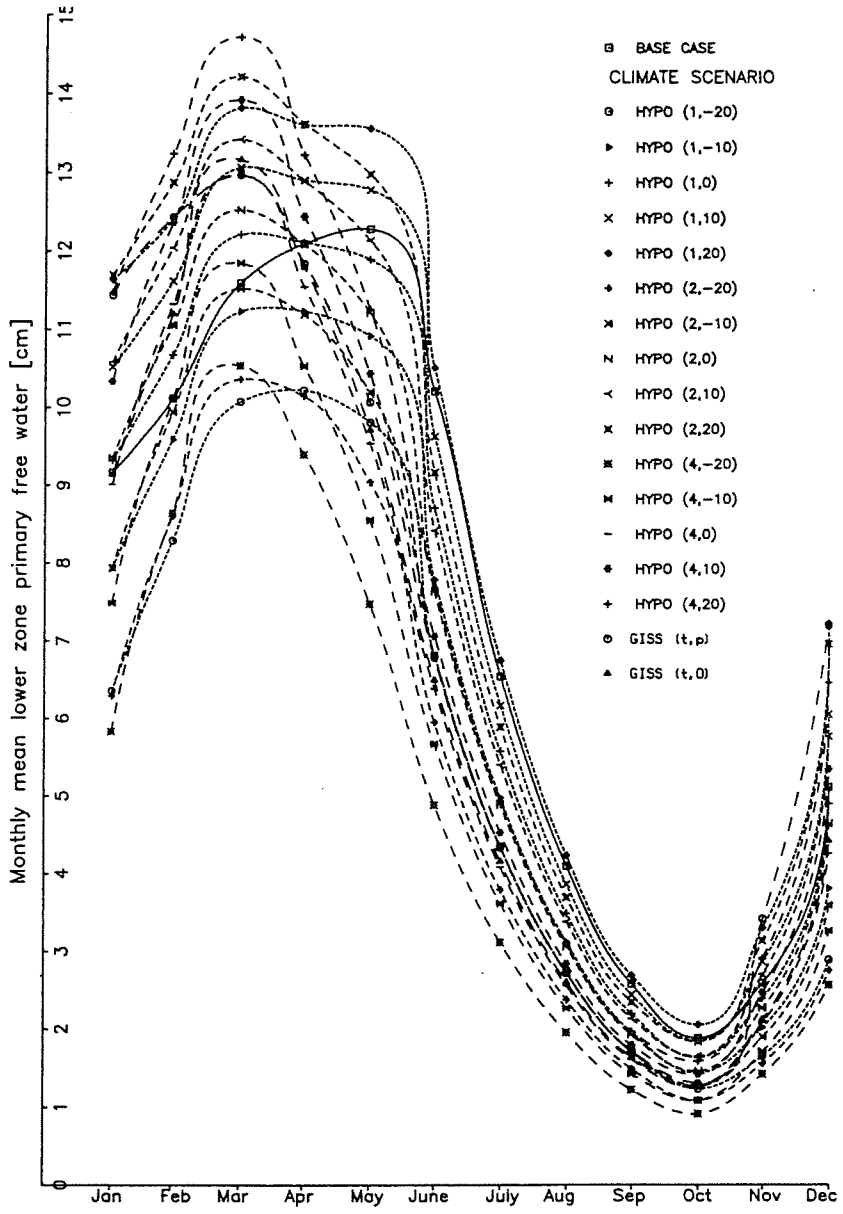

Figure 11-8. Mesochora catchment monthly mean lower zone primary free water for the HYPO, GISS and base case climate scenarios

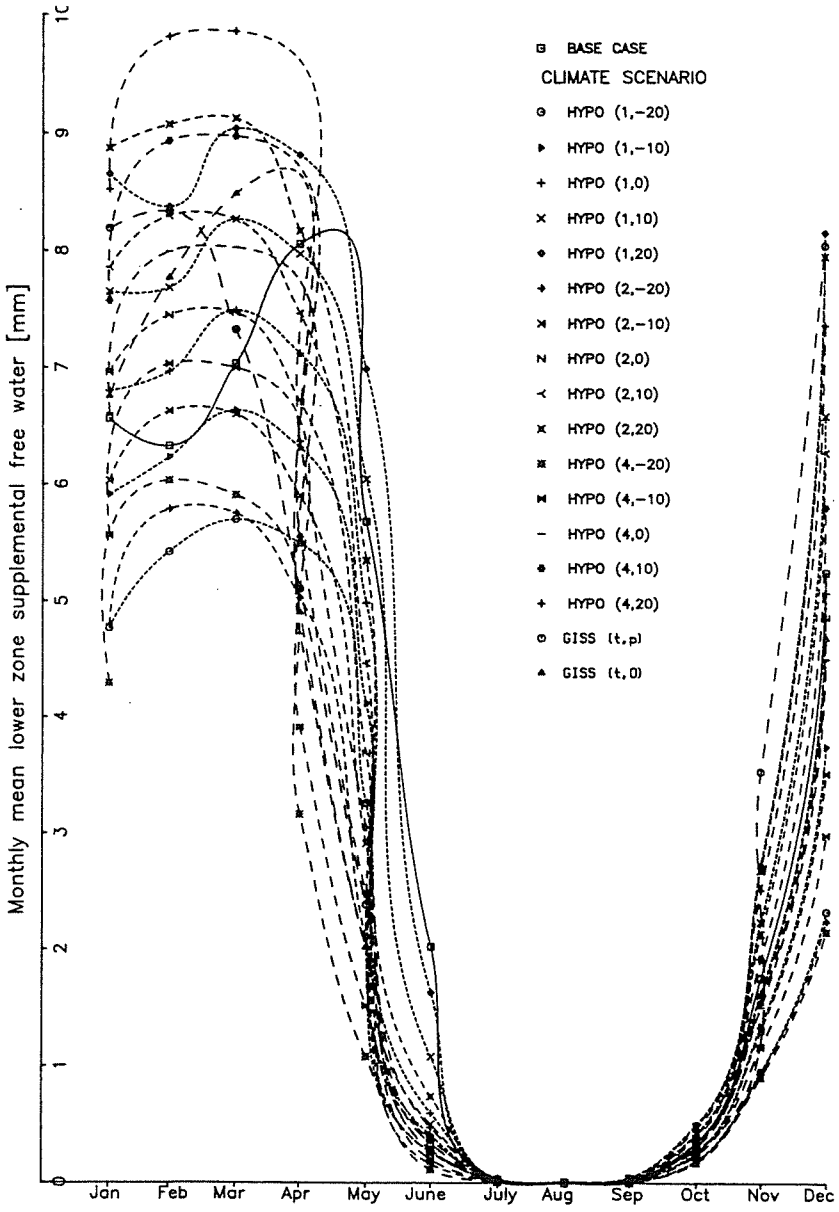

Figure 11-9. Mesochora catchment monthly mean lower zone supplemental free water for the HYPO, GISS and base case climate scenarios

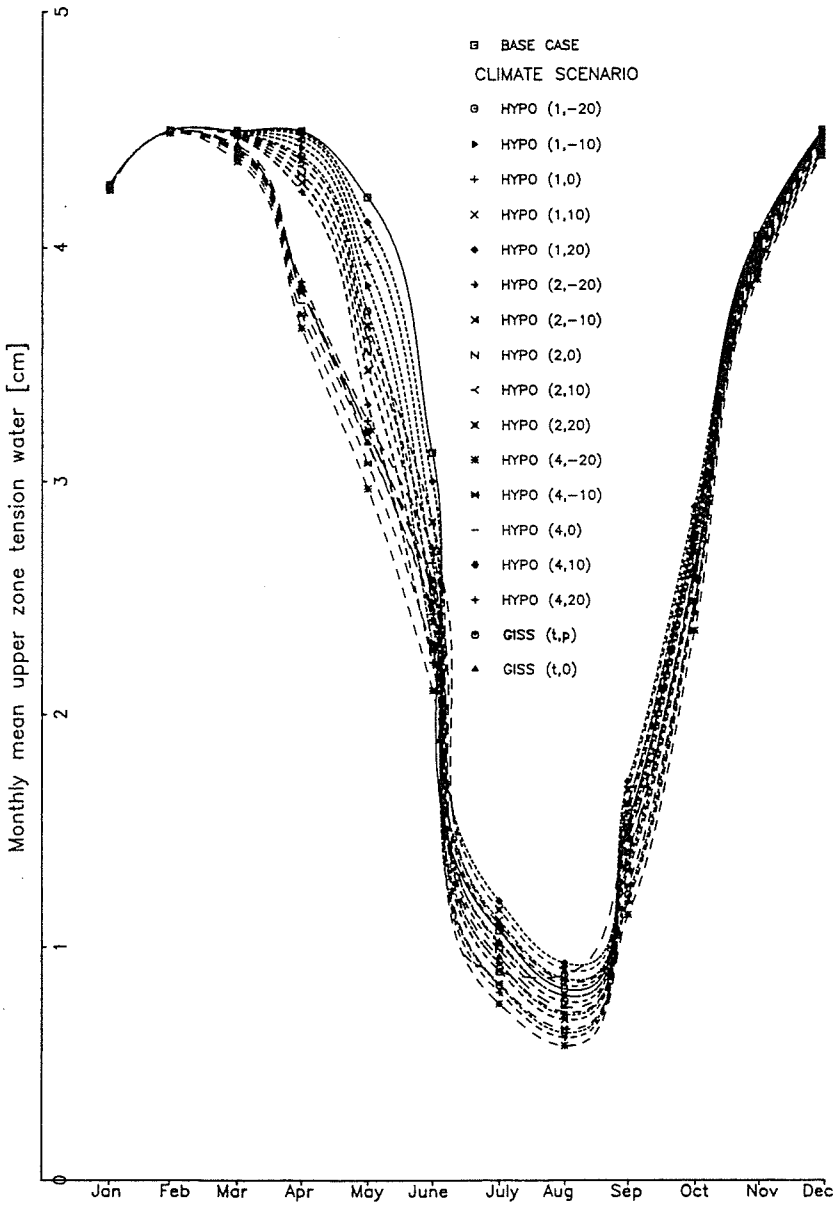

Figure 11-10. Mesochora catchment monthly mean upper zone tension water for the the HYPO, GISS and base case climate scenarios

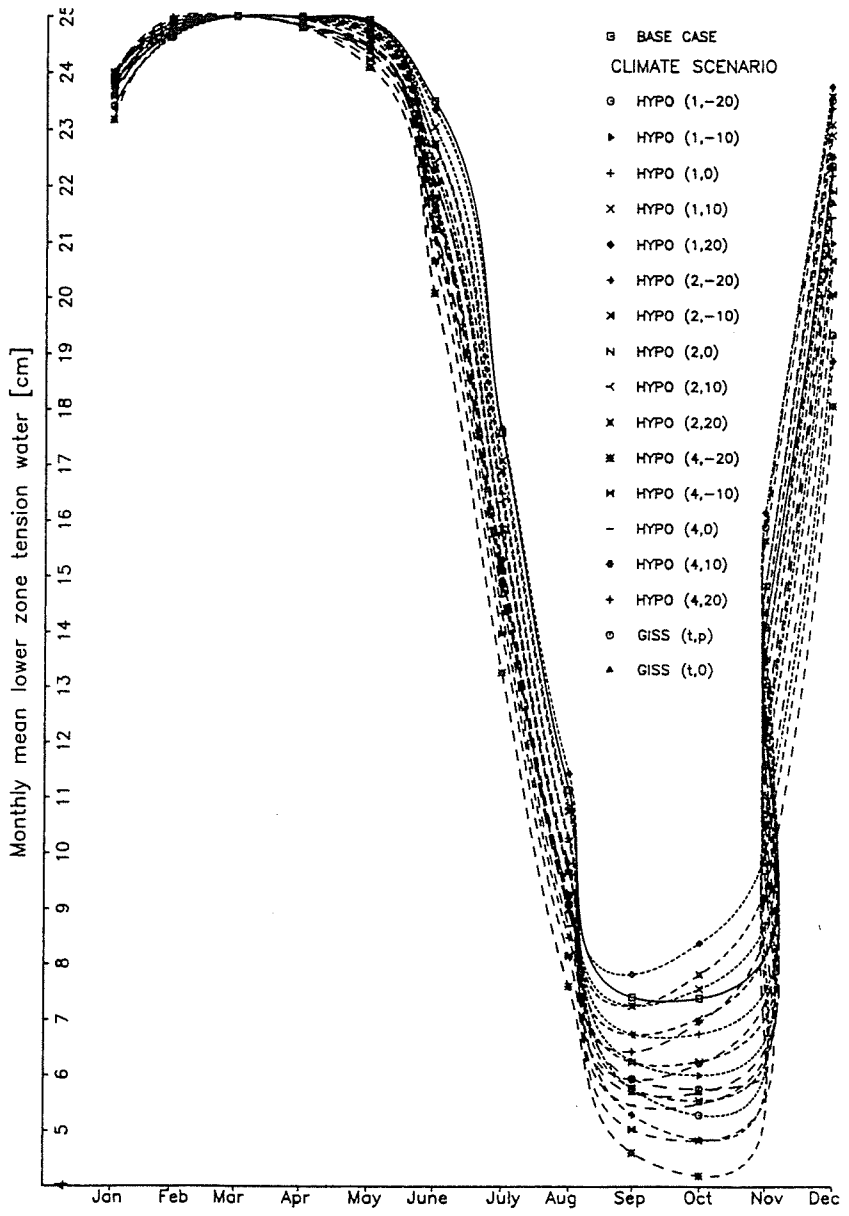

Figure 11-11. Mesochora catchment monthly mean lower zone tension water for the the HYPO, GISS and base case climate scenarios

11-8. CONCLUSIONS

Before jumping to the final conclusions of this research, it is necessary to make clear at this juncture that (a) the simulation results constitute alternative scenarios and not deterministic predictions and (b) because the assumptions and simplification incorporated in the models are reflected in the results, we thought if advisable to elaborate on these assumptions, namely:

a) The application of uniform climate change: Because the precipitation was adjusted for climate change with a fixed factor, this implies that the coefficient of variation (standard deviation divided by the mean) is the same for the altered climate scenarios as for the base case. For precipitation factors greater than one this means that the precipitation and its variability will increase, a fact that could affect the streamflow variability and hence the operation of a given reservoir or the design of new facilities.
b) The capability of hydrological models to provide a sufficient description of the catchment dynamics to altered climates: Although the NWS models contain the appropriate level of detailed dynamics for medium-sized catchments and can also capture the basic elements of the long-term hydrological response of the catchment, their adaptability to altered climates is rather difficult to determine. The parameters of the soil moisture accounting model are climate- dependent and hence their yields for altered inputs are strongly model- dependent. Another major problem of this model is that it cannot possibly be relied on long-term changes in vegetation (Panagoulia, 1994).

Having considered the limitations imposed by the various assumptions, the following general conclusions can be reached, viz:

a) The monthly distribution patterns of the catchment hydrological variables for HYPO and GISS climate scenarios are very alike.
b) Both the HYPO and GISS temperature increases associated with all precipitation changes, could possibly cause substantial decreases in average snow accumulations.
c) Reduction in the amount of precipitation that is falling like snow could increase the winter runoff volumes and decrease the summer and spring runoff ones, thus causing the floods to rise in winter and water shortages to occur in summer.
d) Increased precipitation falling like rain in the winter could possibly increase the winter soil moisture storages, thereby making much more moisture available for actual evapotranspiration in the early spring. Increased temperatures could increase the spring's actual evapotranspiration.
e) The reduction in moisture supplied in the form of snowmelt in spring combined with increased spring actual evapotranspiration could reduce the soil moisture of late spring, summer and fall, which could in turn reduce runoff during these periods.
f) Significant differences were noted in hydrological numerical results among the two GISS scenarios and HYPO scenarios due to the wide range of the climate variables changes (e.g. the GISS precipitation increase in October was up 50%).

Acknowledgment

I thank sincerely the civil engineer George Dimou who helped me enormously in computer themes.

REFERENCES

Allen R.G., Smith M., Perrier A., and Pereira L.S. (1994). Updated Reference Evapotranspirartion Definition and Calculation Procedures. ICIC Bulletin .

Anderson E.A. (1973). National Weather Service river forecast system. Snow accumulation and ablation model NOAA Technical Memorandum NWS HYDRO 17.

Becker A. and Nemec J.(1987). Macroscale hydrologic models in support to climate research. The Influence of Climate Change and Climatic Variability on the Hydrologic Regime and Water Resources, Proceedings of the Vancouver Symposium, August 1987. IAHS Publ. no. 168: 431-445.

Budyko M.I.(1989). Climatic conditions of the future. Conference on Climate and Water, Helsinki, National IHP Committee Finland, 9-30.

Burnash R.J.C., Ferral R.L., and Mcquire R.A. (1973). A generalized streamflow simulation system conceptual modelling for digital computers. U.S. National Weather Service, Sacramento, CA.

Dickinson R.E. (1982). Modelling climate change due to carbon dioxide increases. *In*: W.C. Clark, (ed.), Carbon Dioxide Review. Oxford University Press, New York.

Doorenbos, J. and Pruitt W.O. (1977). Guidelines for predicting crop water requirements. Irrigation and Drainage Paper 24, 2nd Ed. FAO, Rome, pp. 156.

Georgakakos K.P. and Krajewski W.F. (1991). Worth of radar data in the real- time prediction of mean areal rainfall by nonadvective physically models Water Resour. Res., 27(2): 185-197.

Gleick P.H.(1986). Regional water availability and global climatic changes: The hydrologic consequences of increases in atmospheric CO_2 and other trace gases. Energy and Resources Group, PhD Thesis ERG-DS 86-1, University of California, Berkeley, California, USA.

Hansen J., Russell G., Rind D., Stone P., Laus A., Lebedeff S., Ruedy R., and Travis L. (1983). Efficient three-dimensional global models for climate studies: Models I and II. Monthly Weather Review, 111(4): 609-662.

Hansen J., Fung I., Laus A., Rind D., Lebedeff S. Rueddy R. Russel G., and Stone P. (1988). Global climate changes as forecast by Goddard Institute for space studies three-dimensional model. J. Geophys. Res., 93 (D8): 9341-9364.

Hutchinson M.F. (1990). A point rainfall model based on a three-state continuous Markov occurence process J. Hydrology, 114: 125-148.

Jensen M.E., Burman R.D., and Allen (1990). Evapotranspiration and Irrigation Water Requirements. ASCE Manuals and Reports on Engineering Practices No 70. American Society of Civil Engineers. New York, pp. 442.

Lettenmaier D.P. and Gan T.Y. (1990). Hydrologic sensitivities of the Sacramento-San Joaquin River Basin, California, to global warming. Water Resour. Res. 26(1): 69-86.

Linsley R.K., Kohler Max A., and Paulhus J.L.H. (1988). Hydrology for Engineers, McGraw-Hill, N.Y.

MacCracken M. and Luther F. (Ed.). (1986). Projecting the climatic effects of increasing carbon dioxide. U.S. Office of Energy Research, Office of Basic Energy Sciences. Carbon Dioxide Research Division Washington, D.C.

Manabe S. and Wetherald R. (1985). CO_2 and hydrology. *In*: Advances in Geophysics. 28(a). Academic Press, Washington, D.C.

Mitchell J.F.B. and Qingcum Z. (1991). Climate change prediction. *In*: Climate Change: Science, Impacts and Policy, Proceedings of the Second World Climate Conference, Geneva, October-November 1990. J.Jager and H.L. Ferguson (Eds), pp. 59-70.

Nemec J. and Schaake J. (1982). Sensitivity of water resources systems to climate variation. Hydrological Sciences, 27(3): 327-343.

Panagoulia D. and Dimou G. (1994). Temporal scale effects on modelled catchment hydrological processes in respect of global climate change. Western Pacific Geophysics Meeting, AGV, Book of Abstracts 30, Hong Kong, July 25-29, 1994.

Panagoulia D. (1994). Global climate changes and water resources decision- making, Second European Conference on Advances in Water Resources Technology and Management, Lisbon Portugal, 14-18 June 1994.

Panagoulia D. (1993a). Catchment hydrological responses to climate changes calculated from incomplete climatological data, Proceedings of Exchange Processes at the Land Surface for a Range of Space and Time Scales, IAHS Publications, No 212, Yokohama Japan, 13-16 July, pp. 461-468.

Panagoulia D. (1993b). Documentation of global climate changes through catchment hydrological modelling. *In*: NATO Proceedings of Engineering Risk and Reliability in a Changing Physical Environment, May 24-June 4, Deauville, France.

Panagoulia D. (1992a). Hydrological modelling of a medium-sized mountainous catchment from incomplete meteorological data. J. Hydrol., 137: 1-4, 279-310.

Panagoulia D. (1992b). Impacts of GISS-modelled climate changes on catchment hydrology. Hydrol. Sci. J., 37(2): 141-163.

Panagoulia D. (1991a). Hydrological response of a medium-sized mountainous catchment to climate changes. Hydrol. Sci. J., 36(6): 525-547.

Panagoulia D. (1991b). A technique estimating daily catchment precipitation with elevation correction for conceptual simulation. *In:* Proc. Advances in Water Resources Technology, Published for ECOWARM by A.A.Balkema, Athens, Greece, pp. 89- 101.

Panagoulia D. (1990). Sensitivity Analysis of Catchment Hydrological Response to Climate Changes. PhD Thesis, National Technical University of Athens, Greece.

Peck E.L. (1976). Catchment modelling and initial parameter estimation for the National Weather Service Forecast System. NOAA Techn. Memorandum NWS HYDRO 31.

Revelle R.R. and Waggoner, R.E. (1983). Effects of a carbon dioxide-induced climatic change on water supplies in the Western United States. *In*: Changing Climate, National Academy of Sciences. National Academy Press, Washington D.C.

US. National Academy of Sciences (1983). Changing climate. National Academy of Sciences, National Academy Press, Washington D.C., USA.

US. National Academy of Sciences (1977). Climate, Climatic Change and Water Supply - Overview and Recommendations, 1-23, National Academy of Sciences, Washington D.C., USA.

Wallis J.R., Lettenmaier D.P., and Wood, E.F. (1991). A daily hydroclimatological data set for the Continental United States. Water Resour. Res., 27(7): 1657-1663.

Veihmeyer F.J. (1964). Evapotranspiration. *In*: Handbook of Applied Hydrology, V.T. Chow. (Ed.), McGraw Hill, New York.